Desalination and Water Treatment
www.deswater.com

doi: 10.1080/19443994.2016.1173596

57 (2016) 27409–27418
December

Taylor & Francis
Taylor & Francis Group

Biosorption of aqueous lead and nickel by solvent-free synthesized flake-like polysaccharide resin

Mostafa Hossein Beyki[a], Hassan Alijani[b], Yousef Fazli[c,*]

[a]*School of Chemistry, University College of Science, University of Tehran, P.O. Box 14155-6455, Tehran, Iran, email: hosseinbakim@gmail.com*
[b]*Department of Chemistry, Amirkabir University of Technology (Tehran Polytechnic), P.O. Box 15875-4413, Tehran, Iran, email: Alijani.hassan89@gmail.com*
[c]*Faculty of Science, Department of Chemistry, Islamic Azad University, Arak Branch, Arak, Iran, Tel./Fax: +98 86 33670017; emails: yousef.fazli@gmail.com, y-fazli@iau-arak.ac.ir*

Received 30 October 2015; Accepted 15 March 2016

ABSTRACT

We report the solvent-free synthesis of flake-like polysaccharide-based resin from sugar and phtalic anhydride as solid raw reagents. Prepared material was characterized by Fourier transform infrared spectra, scanning electron microscopy, transmission electron microscopy, XRD, X-ray spectrometry, and thermal gravimetric analysis techniques and was employed as a green adsorbent for removing aqueous lead and nickel. Equilibrium was obtained after 15 min and adsorption followed second-order kinetic model. Isotherm and thermodynamic studies showed that metal adsorption followed Langmuir model and endothermic path. Regeneration study indicated that the adsorbed ions can be released by eluting with 0.5 mol L^{-1} of HCl solution.

Keywords: Lead; Nickel; Polysaccharide; Resin

1. Introduction

The presence of heavy metal ions, i.e. Ni, Pb, Zn, Cu, etc. in the environment is of major concern due to their toxicity to many life forms [1]. As they are not degradable, and exposure even at trace level is believed to be a risk for human beings. Mining, tannery, jewelry, chemical, metallurgical, electrical, and electronics and also arts and crafts are the main source for metal containing waste pollution [2,3]. As a result, there is a need to develop technologies that can remove toxic heavy metal ions found in wastewater and industrial effluents [4]. Various methods for the removal of toxic metals from an aqueous system have been developed such as ion exchange, reverse osmosis, membrane filtration, complexation–precipitation, and adsorption [5]. Normally, sorption by metal oxide, clay, carbon nanotube and organic sorbents are worldwide adopted in this field since it provides an effective, environmentally friendly, inexpensive, and easy way for environmental remediation [6–11]. In recent decades, efforts have been made to develop low-cost adsorbents, for the removal of heavy metal from aqueous solutions. Hence, natural materials are under consideration for the adsorption of heavy metals, such as egg shell membrane, fly ash, dead biomass

*Corresponding author.

and many others [12,13]. Biosorption for the industrial treatment of pollutants which uses natural products with life source, is still under research and development. Some of the studied biosorbents include tannin-rich materials, cellulose, chitosan, peat moss, rice husks and sawdust. The adsorption of heavy metals by these materials might be attributed to carboxyl, hydroxyl and amino groups that can bind metal ions [14,15].

In comparison with natural compounds, the synthetic materials, especially nanomaterials, could bring better performance and versatility because their physiochemical properties can be easily manipulated. There is a wide variety of techniques for producing nanomaterials, which fall into the three main categories, i.e. vapor condensation, chemical synthesis and biological methods [16]. Despite the usefulness of the methods they have some disadvantages which not only increase the cost but also result in safety and environmental concerns. Recently, solid state solvent free processing was successfully developed for synthesis or functionalization of nanomaterials [17–19]. These techniques may be considered as efficient renewable routes to prepare or modify nanomaterials, but they use and generate substances that possess toxicity to human health and the environment as a result, selection of environment compatible reactants are more desirable.

Based on the noticed cases, we have prepared cross-linked saccharide based resin through thermal reformation of sugar in the presence of phtalic anhydride as cross-linker. In order to investigate the potential activity of as synthesized material for environmental remediation, the available basic centers of the green sorbent have been used for adsorption of divalent lead and nickel from aqueous solutions. Kinetic, isotherm and thermodynamic parameters were also calculated and discussed in detail. This work presents some notable advantages relative to conventional systems. In fact a simple solvent free route has been employed to prepare green sorbent using solid raw materials. Sugar was used as basic reactant. It is known that the mentioned substance has natural source and is being dominantly employed as a flavoring and preservative in candy, food and beverages. Therefore, it can be concluded that the final product possesses little toxicity to ecological systems and human being and can be considered as a green material for environmental remediation purposes. Moreover, the synthetic procedure is free of harmful gases, and does not generate any waste, and thus can be considered as a green way to prepare polymeric resin.

2. Experimental

2.1. Materials

Phtalic anhydride (Merck, Darmstadt, Germany) was applied to preparing polysaccharide. Sugar was supplied from local market in Tehran, Iran. Standard solutions of heavy metal ions (1,000 mg L^{-1}) were prepared by dissolving nitrate salt in a minimum amount of HNO_3 and then diluted to appropriate volume with distilled water. The pH adjustment was performed with 0.1 mol L^{-1} of HCl and NH_3.

2.2. Instruments

The prepared particles were characterized by powder X-ray diffraction analysis using a Phillips powder diffractometer, X′ Pert MPD, with Cu-Ka (λ = 1.540589 Å) radiation in 2θ range of 2°–100°. Field emission scanning electron microscopy (FE-SEM) and transmission electron microscopy (TEM) analysis carried out using HITACHI S 4160 and Zeiss-EM10C instruments. Fourier transform infrared spectra (FT-IR) were measured with Equinox 55 Bruker with attenuated total reflectance method over the wavelength of 400–4,000 cm^{-1}. Thermal gravimetric analysis (TGA) results and energy dispersive X-ray spectrometry (EDX) are recorded with a TA-Q–50 and Oxford ED-2000 (England), respectively. A digital pH-meter (model 692, metrohm, Herisau, Switzerland), was used for the pH adjustment. A Varian model AA-400 flame atomic absorption (FAAS) spectrometer (Varian Australia Pty Ltd, Musgrave), equipped with a deuterium lamp background and hollow cathode lamp, was used for determination of metal ions.

2.3. Synthesis of polysaccharide

Polysaccharide was fabricated by solvent free rout with solid reagents. In a typical run, 1.0 g of sugar and 0.5 g of phtalic anhydride were mixed for 10 min and the mixture was heated at 180°C for 1 h and then further heated at 220°C for 2 h. After cooling to room temperature, it was ground and stored for subsequent work.

2.4. Metal adsorption experiment

Metal adsorption experiments were performed with batch method. For this purpose, different concentrations of lead and nickel ions (0.05–50 mg L^{-1}) were placed in 50-mL volumetric flasks. The pH of the solutions was adjusted and 10 mg of the sorbent was

added to each flask. After shaking for 15 min, the solid mass was collected and the concentration of ions in supernatant was determined by FAAS.

3. Results and discussion

3.1. Characterization of resin

Structure of the resin was characterized by EDX, XRD, FT-IR, TGA, FE-SEM, and TEM analysis. EDX analysis (Fig. 1(a)) showed carbon and oxygen as the only component of polysaccharide and no further element was detected which revealed that the resin has good purity. The XRD analysis was used to verify the crystallinity of resin. The pattern (Fig. 1(b)) showed a main broad scattering beginning from 10° to 50° with a maximum height at 17.4°. These peaks can be assigned to a mixture of cellulose lattice planes corresponding to (0 0 1), (1 0 0), and (1 0 1, 0 0 2) [20]. In the IR spectrum of sugar (Fig. 1(c)), a strong peak at 3,342 cm^{-1} corresponding to the stretching vibration of free –OH groups and the peak at 2,940 cm^{-1} are attributed to the stretching vibration of –CH groups in five and six-membered ring of sugar. The peaks observed at 550–650 and 1,000–1,500 cm^{-1} are due to the bending vibration of CH_2 groups and symmetric stretching vibrations of C–OH of alcoholic groups. After deformation and cross-linking reaction a new peak appeared at around 1,670–1,720 cm^{-1} owing to C=C and C=O vibration. Moreover, wide peak around 1,000–1,300 and 2,500–3,500 cm^{-1} region corresponds to –C–O and –COOH vibration [21]. The TGA pattern of the as-prepared polysaccharide (Fig. 1(d)) shows thermal degradation at two stages, one at 20–100°C with a 5% loss and another at 150–600°C with a 46.5% loss in the resin mass. The first weight loss is due to the volatile low molecular weight compounds which generated as a result of fragmentation reactions in synthesis step, and the second loss is due to the decomposition of the resin. The DTA graph shows

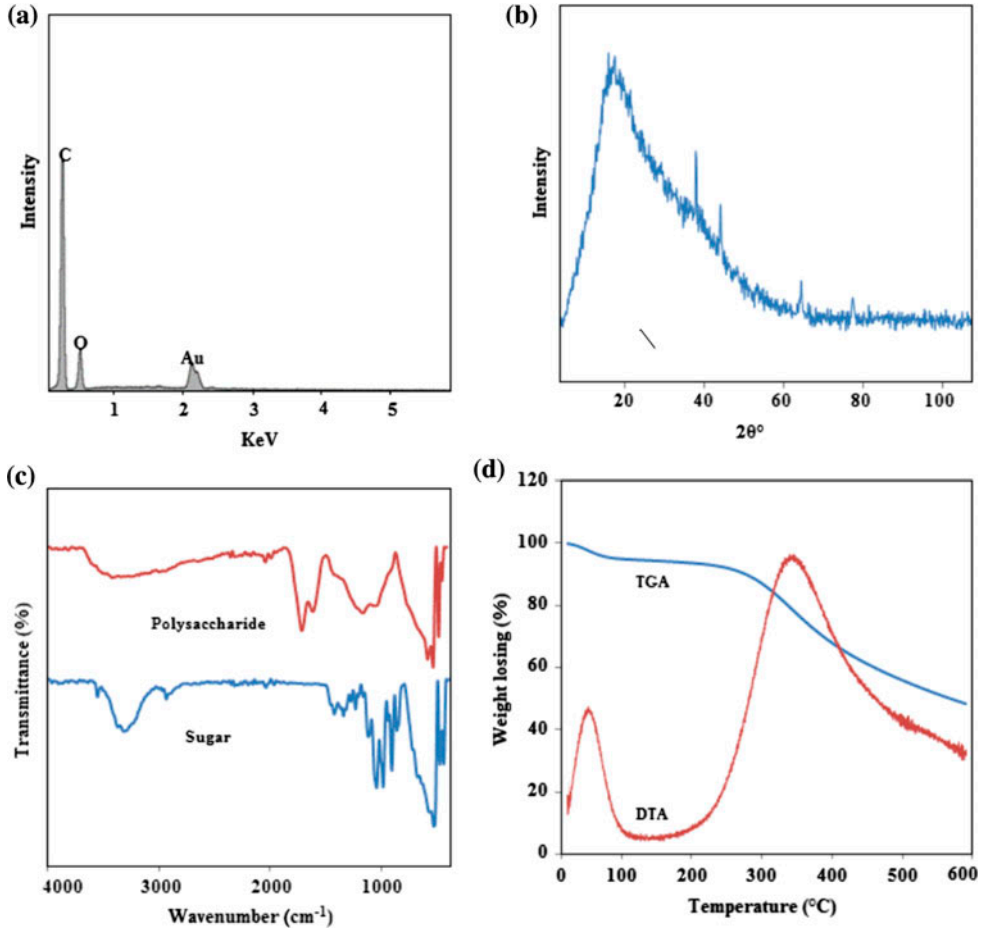

Fig. 1. The EDX spectra (a), XRD pattern (b), FT-IR spectra (c), and TGA–DTA profile (d) of as synthesised polysaccharide resin.

one strong peak around 340˚C which initiated from 250˚C and continued to 600˚C. Broad peak confirm that the polysaccharide composed of fragments with different size as well as high degree of interference of the resin branches in the thermal degradation process. Moreover, the differences in resin species mainly result in different degradation rates [22,23]. FE-SEM image (Fig. 2(a)–(c)) showed irregular stacked flakes with some pore in polysaccharide structure. Further study with TEM analysis (Fig. 2(d)–(f)) proves that polysaccharide has tump lamellar layer as a result of esterification between acid–hydroxyl functional groups in various direction. However, the flakes did not show regular area and thickness but it is evident that their areas are at micro and nanolevels with thickness in nanoscale. It can be seen that the TEM results are in good agreement with the TGA analysis. In other words, as synthesized material composed of irregular fragments which showed different thermal stability as a result of different cross-linking degree.

Saccharose, α-D-glucopyranosyl-(1,2)-β-D-fructofuranoside) is a disaccharide combination of glucose and fructose. By heating of sugars slowly to around 170–180˚C it enters caramelization process. This process includes the removal of water from a sugar, prior to polymerization into high-molecular-weight compounds which possess dark brown color. Other degradation process includes hydrolysis which breaks the glycosidic bond of sugar and converts it into glucose and fructose. This process can be accelerated with acids; hence, phtalic acid exerts two roles in polysaccharide preparation. First, it acts as a cross-linker to link saccharose through esterification reaction. Second, it induces hydroxymethylfurfural formation from sugar which consists of a furan ring, containing both aldehyde and alcohol functional groups [24]. This monomer can also participate in polymerization process through reaction with anhydride and saccharose.

3.2. Effect of pH on metal adsorption

The lead and nickel adsorption experiments were performed at various pH by shaking 10 mg of the sorbent with 50 mL of the ion solution (5 mg L^{-1}) for 5 min and the removal percent (%R) was calculated.

$$\%R = 100\ (C_0 - C_e)/C_0 \tag{1}$$

where C_0 and C_e are initial and equilibrium concentrations of metal ions, respectively. According to Fig. 3(a), the adsorption of both metal ions increases with increasing in pH. Lead adsorption reached to maximum level (76%) at pH 6, while, nickel ions showed maximum removal of 98% at pH 9. Low removal efficiency at acidic solutions is owing to the fact that by decreasing the pH value, the functional groups of sorbent are more protonated and hence,

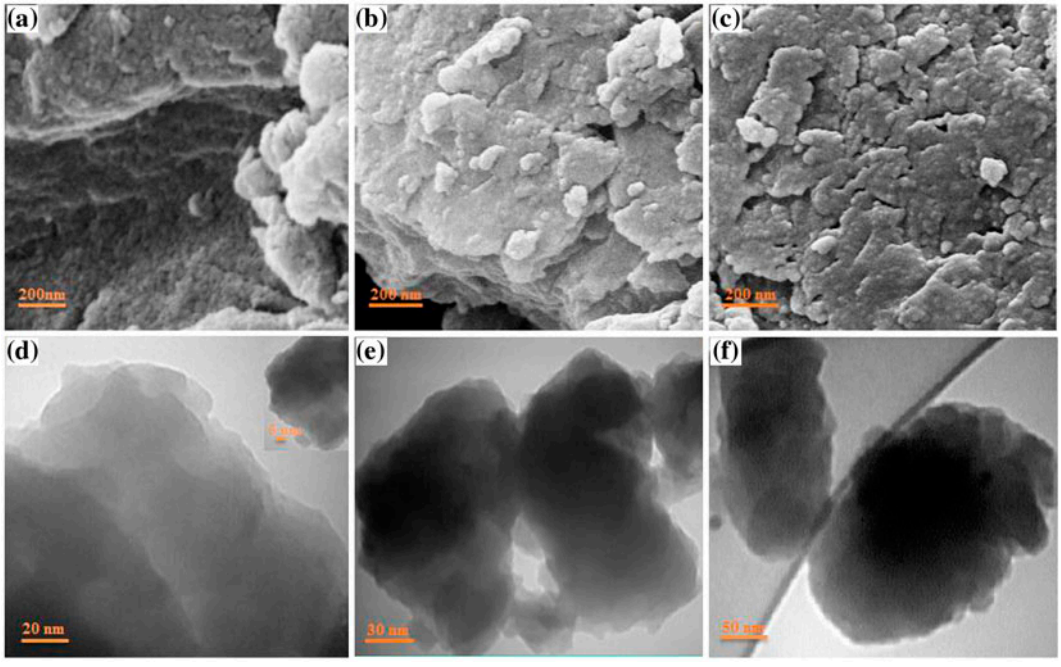

Fig. 2. The FE-SEM (a–c) and TEM (d–f) images of as synthesized polysaccharide resin.

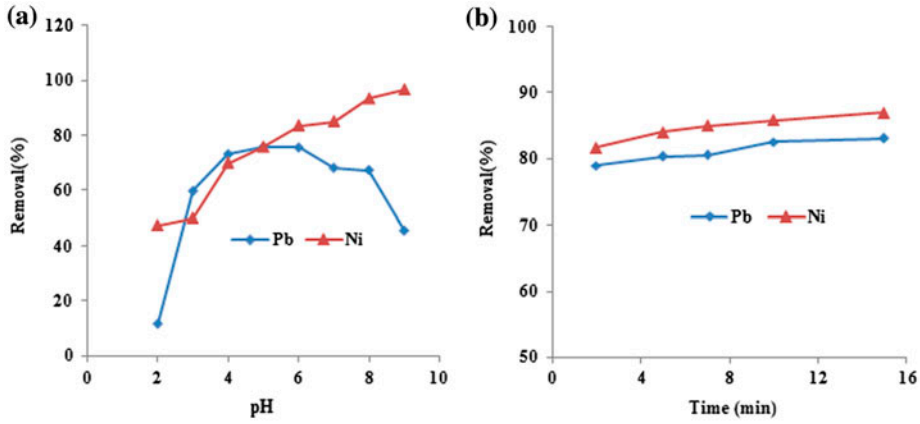

Fig. 3. Effect of pH (a) and time (b) on heavy metal adsorption using the polysaccharide resin. Conditions: volume; 50 mL, adsorbent; 10 mg, metal concentration; 5 mg L^{-1}, shacking time; 5 min.

they are less available to retain the ions. Decrease in lead removal efficiency at pH greater than six, can be as a result of hydroxide formation which hinder effective interaction of lead with the sorbent's functional groups. Nickel ions form amine complexes, $Ni(NH_3)_6^{2+}$; hence, precipitation cannot restrict their adsorption on the sorbent's surface. In consequence, pH of 6 was selected as a working value at subsequent experiments.

3.3. Effect of time and kinetic models

Lead and nickel adsorption on the adsorbent in the concentration level of 5.0 mg L^{-1} was performed within 2–15 min (Fig. 3(b)). Due to the availability of a large number of adsorption sites, the removal was more than 70% at the first two min and then, slowed down as the sites are gradually filled up. In this step, the kinetics will be more dependent on the rate at which the analyte is transported from the liquid phase to the adsorption sites. The increase in removal percent was not significant after 15 min; hence, this time was selected for further works.

To further evaluate the effect of time on lead and nickel adsorption and quantify the changes in adsorption with time, the pseudo-first-order and pseudo-second-order models (Eqs. (2) and (3)) were applied. These models can be represented with the following linear forms:

$$\ln(Q_e - Q_t) = \ln Q_e - K_1 t \quad (2)$$

$$t/Q_t = 1/(K_2\, Q_e^2) + (1/Q_e)\, t \quad (3)$$

where k_1, k_2, Q_e, and Q_t are the pseudo-first-order adsorption rate constant (min^{-1}), the second-order rate constant (g mg^{-1} min^{-1}), the values of the amount adsorbed per unit mass at equilibrium and at any time, t, respectively [25,26]. According to the kinetic plots in Fig. 4(a)–(d), both first- and second-order model for nickel ions have good linearity; however, first-order model for lead adsorption does not have good linearity. Besides, the results in Table 1 showed that the Q_e obtained based on the first-order model has high deviation from experimental value, while for second-order model the deviation is low. Hence, chemisorptions can be accepted as the kinetic mechanism for lead and nickel adsorption.

3.4. Isotherm study

The effect of lead and nickel concentrations on adsorption process was analyzed in terms of Langmuir isotherm which assumes all the sorption sites are energetically the same. This model can be expressed as:

$$C_e/Q_e = 1/Q_m\, b + C_e/Q_m \quad (4)$$

where C_e is amount of metal ions in the liquid phase at equilibrium (mg L^{-1}) and Q_e is the amount of metal ions sorbed per unit mass of the sorbent (mg g^{-1}). The Q_m is maximum adsorption capacity and b is the Langmuir coefficient [27].

The Freundlich model which assumes multilayer adsorption is represented as:

$$Q_e = K_f\, C_e^{1/n} \quad (5)$$

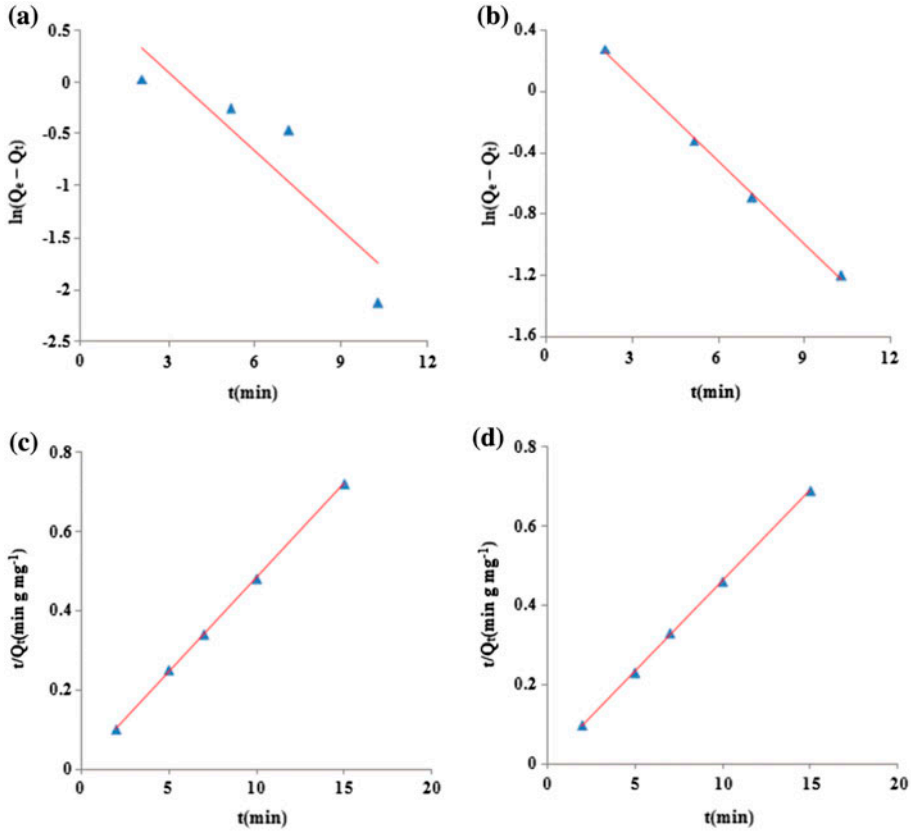

Fig. 4. A typical linear first and second order kinetic plots for lead (a and c) and nickel (b and d). Conditions: pH 6, volume; 50 mL, adsorbent; 10 mg; concentration; 5.0 mg L^{-1}.

Table 1
The data of kinetic models for adsorption of nickel and lead using polysaccharide

Model	Coefficients	Ni^{2+}	Pb^{2+}
First-order	R^2	0.99	0.81
	K_1	0.18	0.26
	Q_t (mg g^{-1})	9.87	16.08
Second-order	R^2	0.99	0.99
	K_2	0.40	0.31
	Q_t (mg g^{-1})	22.22	21.27
	Q_{exp} (mg g^{-1})	20.77	20.77

where n and K_f are the Freundlich coefficients which evaluated from the slopes and intercepts of linear plot [28,29]. The graph for the isotherm models are depicted in Fig. 5, and results are listed in Table 2 which showed that the maximum adsorption capacity of polysaccharide is 66.6 and 58.8 mg g^{-1} for lead and nickel, respectively. As seen from results, both Freundlich and Langmuir isotherms fit well with the experimental data. It is known that Freundlich model shows that adsorption-complexation reactions taking place in the adsorption process as well as active sites homogeneously distributed on the sorbent surface; however, the Langmuir isotherm corresponds to a dominant ion exchange mechanism. As a result both adsorption–complexation and ion exchange are responsible for the metal removal. These results indicate that the mechanism of lead and nickel adsorption is complex and follows physicochemical mechanism. The accuracy of the isotherm models was further evaluated by a chi-square test (χ^2) [30,31]. This error function is given as followed:

$$\chi^2 = \sum \frac{(Q_{exp} - Q_c)^2}{Q_c} \quad (6)$$

where Q_{exp} and Q_c are the experimental data and that calculated from the non-linear model. Based on the results given in Table 2, the Langmuir model has a lower χ^2 value and reveals that this model can better describe the adsorption behavior of the sorbent. To further evaluate adsorption behavior of the resin, nickel and lead adsorption was performed at high

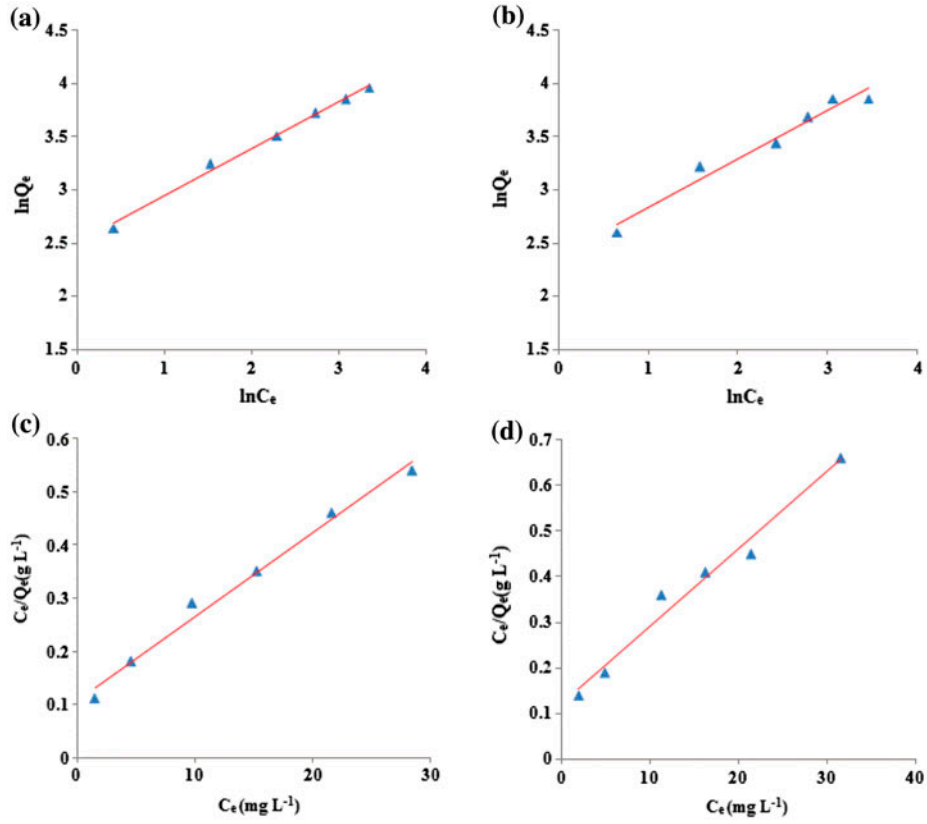

Fig. 5. Freundlich and Langmuir plots for lead (a and c) and nickel (b and d) Conditions: volume; 50 mL, pH 6, time; 15 min, adsorbent; 10 mg; concentration 10–60 mg L^{-1}.

Table 2
The data of isotherms for lead and nickel adsorption using the polysaccharide

		Lead		Nickel	
	C_0 (mg L^{-1})	100–500	10–60	100–500	10–60
Langmuir	Q_m (mg g^{-1})	74.0	66.6	63.5	58.8
	R^2	0.97	0.99	0.93	0.97
	b	0.12	0.14	0.09	0.14
	χ^2	5.2	3.6	4.2	2.5
Freundlich	n	1.7	2.27	2.2	2.17
	K_f	145	132	115	103
	R^2	0.98	0.99	0.96	0.96
	χ^2	2.7	4.4	1.3	3.0

concentrations (100–500 mg L^{-1}). Results at Table 2, show that the adsorption behavior has been reversed because the Freundlich model well fitted with the experimental values.

3.5. Thermodynamic study

To evaluate effect of temperature on lead and nickel adsorption the experiments were performed at the temperature of 294, 308, and 321 K with initial metal concentration of 10 mg L^{-1} and adsorbent dosage of 10 mg. It was observed that with increase in reaction temperature the adsorption removal was increased which indicate that the adsorption on adsorbent obeys endothermic path. The standard thermodynamic parameters for the adsorption process, ΔH°, ΔS°, and ΔG° (kJ mol^{-1}) could be evaluated using the following equations [32]:

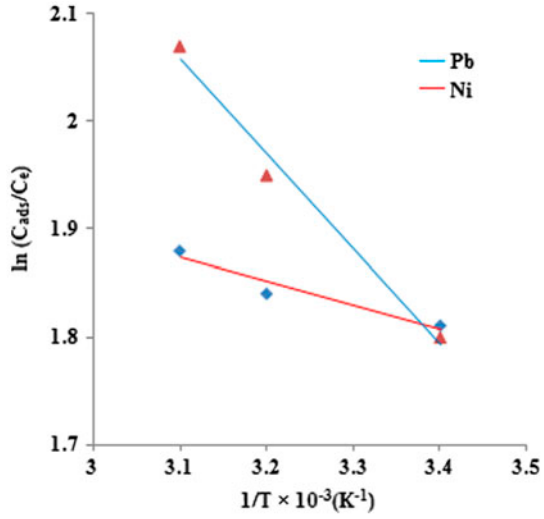

Fig. 6. The relationship curve between $\ln(C_{ads}/C_e)$ and $1/T$. Conditions: volume; 50 mL, time; 15 min, adsorbent; 10 mg, concentration10 mg L^{-1}.

$$\Delta G^\circ = -RT \ln (C_{ads}/C_e) \quad (7)$$

$$\Delta G^\circ = \Delta H^\circ - T\Delta S^\circ \quad (8)$$

$$\ln(C_{ads}/C_e) = \Delta S^\circ/R - \Delta H^\circ/RT \quad (9)$$

where R and T are gas constant (8.314×10^{-3} kJ K^{-1} mol^{-1}) and absolute temperature (K), respectively [33]. Moreover, C_{ads} (mg L^{-1}) is the amount of lead and nickel adsorbed onto adsorbent at equilibrium, and C_e (mg L^{-1}) is the equilibrium concentration of target ions in solution [34,35]. The results in Fig. 6 and Table 3 indicate that with increase in the reaction temperature the value of standard Gibbs energy decreases which indicates that the interaction is spontaneous and suggests that the process is feasible at higher temperatures. The positive value of ΔS° show increase randomness at the solid–solution interface and also indicates that the distribution of metal ions adsorbed by these sorbent was more chaotic than that in the aqueous solution. Moreover, the positive value indicates an affinity of the sorbent toward metal ions [36,37].

3.6. Adsorption mechanism

Lead and nickel adsorption onto polysaccharide may take place through physical or chemical adsorption. The result of kinetic study can exhibit a standpoint about the adsorption mechanism. First order kinetic model represent physical adsorption or ion exchange mechanism; however, second order model is equal to chemisorption. Moreover, according to the isotherm models the Freundlich isotherm correspond to physical adsorption beside Langmuir model shows monolayer chemisorption process. Moreover, it is known that if the heat of sorption was in the range of 2.1–20.9 kJ mol^{-1} the process is physical, while if the heat of sorption is in the range 80–200 kJ/mol, the process is chemisorption [38]. According to the experimental results, metal sorption is not net physical or chemical interaction and is along with a physicochemical sorption process. In other words, the adsorption process followed second order kinetic model and both Langmuir and Freundlich models showed high linearity. Besides, the heat of sorption is 1.8–7.3 kJ mol^{-1} for nickel and lead, respectively. This result indicates that the metal adsorption mechanism is complex and the process followed physiochemical mechanism.

3.7. Desorption and reusability

To make the sorption process more economical, it is necessary to regenerate the sorbent material. For this purpose, different concentrations of HCl (0.1, 0.2, 0.5, and 1.0 mol L^{-1}) were tested to elute the metal ions from sorbent surface. Selection of acid was based on the fact that in acidic solution removal efficiency was low. Observations indicated that by using HCl solution (0.5 mol L^{-1}), desorption was more than 98%. Moreover, it was found that the sorbent has good removal efficiency (70–90%) after five cycles of sorption and desorption.

3.8. Comparison with other methods

In Table 4, the performance of proposed method for nickel and lead adsorption were compared with some reports in literature. Based on the results, the

Table 3
The thermodynamic data for lead and nickel adsorption using as synthesized polysaccharide

	ΔG° (kJ mol^{-1})			ΔH° (kJ mol^{-1})	ΔS° (J k^{-1} mol^{-1})
	294 K	308 K	321 K		
Pb^{2+}	–4.39	–4.99	–5.52	+7.30	+39.74
Ni^{2+}	–4.42	–4.71	–5.01	+1.84	+21.27

Table 4
Comparison of obtained results with other methods for adsorption of nickel and lead by as synthesized polysaccharide

Sorbent	Q_m (mg g^{-1})		Time (min)	Refs.
	Pb^{2+}	Ni^{2+}		
Sawdust	–	9.8	–	[1]
Meranti sawdust	34.2	35.9	120	[3]
Aspergillus niger, biomass	4.7	1.6	240	[4]
Soy protein	235.5	177.1	240	[5]
MWCNTs	10.3	8.9	10	[7]
Sawdust-walnut	6.5	2.4	60	[14]
Magnetite-Kaolinite	106	95.2	120	[27]
Litchi peels	78.7	–	120	[33]
Polysaccharide	66.6	58.8	15	This work

performance of this method was significantly better than the previous ones with respect to the adsorption time. Moreover, the sorbent showed satisfactory adsorption capacity. As a results the proposed system is a good choice for heavy metal removal from aqueous solutions especially that the material can be considered as a green sorbent.

4. Conclusions

In this work, we have developed a sustainable green rout to synthesis of flake-like polysaccharide resin. The method as a highly sustainable way exhibiting the some benefits such as; employment of low-cost nontoxic organic reagents with natural source as well as avoidance of harmful gases that is ecologically beneficial and generates substances that possess low toxicity to human health and the environment. Moreover, prepared resin was employed for fast adsorption of lead and nickel ions from aqueous solution. The retained metal ions can be eluted with the HCl solution; moreover, the adsorbent showed good reusability. Metal-polysaccharide interactions were accompanied by an increase in the ΔS value and an endothermic enthalpy change. Moreover, the kinetics of the interaction has been described by a pseudo-second-order mechanism.

Acknowledgment

Support of this study by the research council of Islamic Azad University, Arak Branch, through grant is gratefully acknowledged.

References

[1] S.R. Shukla, R.S. Pai, Adsorption of Cu(II), Ni(II) and Zn(II) on dye loaded groundnut shells and sawdust, Sep. Purif. Technol. 43 (2005) 1–8.

[2] H. Li, F. Liu, M. Zhu, X. Feng, J. Zhang, H. Yin, Structure and properties of Co-doped cryptomelane and its enhanced removal of Pb^{2+} and Cr^{3+} from wastewater, J. Environ. Sci. 34 (2015) 77–85.

[3] M. Rafatullah, O. Sulaiman, R. Hashim, A. Ahmad, Adsorption of copper (II), chromium (III), nickel (II) and lead (II) ions from aqueous solutions by meranti sawdust, J. Hazard. Mater. 170 (2009) 969–977.

[4] M. Amini, H. Younesi, Biosorption of Cd(II), Ni(II) and Pb(II) from aqueous solution by dried biomass of *Aspergillus niger*: Application of response surface methodology to the optimization of process parameters, CLEAN—Soil Air Water 37 (2009) 776–786.

[5] D. Liu, Z. Li, W. Li, Z. Zhong, J. Xu, J. Ren, Z. Ma, Adsorption behavior of heavy metal ions from aqueous solution by soy protein hollow microspheres, Ind. Eng. Chem. Res. 52 (2013) 11036–11044.

[6] L. Giraldo, A. Erto, J.C. Moreno-Piraján, Magnetite nanoparticles for removal of heavy metals from aqueous solutions: Synthesis and characterization, Adsorption 19 (2013) 465–474.

[7] M. Tuzen, K.O. Saygi, M. Soylak, Solid phase extraction of heavy metal ions in environmental samples on multiwalled carbon nanotubes, J. Hazard. Mater. 152 (2008) 632–639.

[8] T.K. Naiya, A.K. Bhattacharya, S.K. Das, Clarified sludge (basic oxygen furnace sludge)—An adsorbent for removal of Pb(II) from aqueous solutions—Kinetics, thermodynamics and desorption studies, J. Hazard. Mater. 170 (2009) 252–262.

[9] H. Javadian, Adsorption performance of suitable nanostructured novel composite adsorbent of poly (N-methylaniline) for removal of heavy metal from aqueous solutions, J. Ind. Eng. Chem. 20 (2014) 4344–4352.

[10] S. Vellaichamy, K. Palanivelu, Preconcentration and separation of copper, nickel and zinc in aqueous samples by flame atomic absorption spectrometry after column solid-phase extraction onto MWCNTs impregnated with D2EHPA-TOPO mixture, J. Hazard. Mater. 185 (2011) 1131–1139.

[11] G. Zhao, X. Ren, X. Gao, X. Tan, J. Li, C. Chen, Y. Huang, X. Wang, Removal of Pb(ii) ions from aqueous solutions on few-layered graphene oxide nanosheets, Dalton Trans. 40 (2011) 10945–10952.

[12] D. Afzali, S.Z. Mohammadi, Determination trace amounts of copper, nickel, cobalt and manganese ions in water samples after simultaneous separation and preconcentration, Environ. Chem. Lett. 9 (2011) 115–119.
[13] D. Boˇzić, V. Stanković, M. Gorgievski, G. Bogdanović, R. Kovačcević, Adsorption of heavy metal ions by sawdust of deciduous trees, J. Hazard. Mater. 171 (2009) 684–692.
[14] B. Yasemin, T. Zeki, Removal of heavy metals from aqueous solution by sawdust adsorption, J. Environ. Sci. 19 (2007) 160–166.
[15] F. Asadi, H. Shariatmadari, N. Mirghaffari, Modification of rice hull and sawdust sorptive characteristics for remove heavy metals from synthetic solutions and wastewater, J. Hazard. Mater. 154 (2008) 451–458.
[16] A. Kaur, U. Gupta, A review on applications of nanoparticles for the preconcentration of environmental pollutants, J. Mater. Chem. 19 (2009) 8279–8289.
[17] C.A. Dyke, J.M. Tour, Solvent-free functionalization of carbon nanotubes, J. Am. Chem. Soc. 125 (2003) 1156–1157.
[18] P. Siemion, J. Kapuśniak, J.J. Kozioł, Solid-state thermal reactions of starch with semicarbazide hydrochloride. Cationic starches of a new generation, Carbohydr. Polym. 62 (2005) 182–186.
[19] J. Lu, S. Yang, K.M. Ng, C-H. Su, C.-S. Yeh, Y-N. Wu, D-B. Shieh, Solid-state synthesis of monocrystalline iron oxide nanoparticle based ferrofluid suitable for magnetic resonance imaging contrast application, Nanotechnology. 17 (2006) 5812–5820.
[20] M. Bayat, M.H. Beyki, F. Shemirani, One-step and biogenic synthesis of magnetic Fe_3O_4–Fir sawdust composite: Application for selective preconcentration and determination of gold ions, J. Ind. Eng. Chem. 21 (2015) 912–919.
[21] H. Alijani, Z. Shariatinia, A. Aroujalian Mashhadi, Water assisted synthesis of MWCNTs over natural magnetic rock: An effective magnetic adsorbent with enhanced mercury(II) adsorption property, Chem. Eng. J. 281 (2015) 468–481.
[22] M.W. Sabaa, Thermal degradation behaviour of sisal fibers grafted with various vinyl monomers, Polym. Degrad. Stab. 32 (1991) 209–217.
[23] M. Brebu, C. Vasile, Thermal degradation of lignin—A review, Cellul. Chem. Technol. 44 (2010) 353–363.
[24] Y. Roman-Leshkov, J.N. Chheda, J.A. Dumesic, Phase modifiers promote efficient production of hydroxymethylfurfural from fructose, Science 312 (2006) 1933–1937.
[25] S.T. Akar, D. Yilmazer, S. Celik, Y.Y. Balk, T. Akar, Effective biodecolorization potential of surface modified lignocellulosic industrial waste biomass, Chem. Eng. J. 259 (2015) 286–292.
[26] H.-U. Kim, K.-H. Kim, Y.-Y. Chang, S.M. Lee, J-K. Yang, Heavy metal removal from aqueous solution by tannins immobilized on collagen, Desalin. Water Treat. 48 (2012) 1–8.
[27] M.R. Lasheen, I.Y. El-Sherif, D.Y. Sabry, S.T. El-Wakeel, M.F. El-Shahat, Adsorption of heavy metals from aqueous solution by magnetite nanoparticles and magnetite-kaolinite nanocomposite: Equilibrium, isotherm and kinetic study, Desalin. Water Treat. (in press), doi: 10.1080/19443994.2015.1085446.
[28] S. Bekkouche, S. Baup, M. Bouhelassa, S. Molina-Boisseau, C. Petrier, Competitive adsorption of phenol and heavy metal ions onto titanium dioxide (Dugussa P25), Desalin. Water Treat. 37 (2012) 364–372.
[29] L. Mihaly-Cozmuta, A. Mihaly-Cozmuta, A. Peter, C. Nicula, H. Tutu, D. Silipas, E. Indrea, Adsorption of heavy metal cations by Na-clinoptilolite: Equilibrium and selectivity studies, J. Environ. Manage. 137 (2014) 69–80.
[30] T. Kumar Naiya, A. Kumar Bhattacharya, S. Kumar Das, Clarified sludge (basic oxygen furnace sludge)—An adsorbent for removal of Pb(II) from aqueous solutions—Kinetics, thermodynamics and desorption studies, J. Hazard. Mater. 170 (2009) 252–262.
[31] P. Sampranpiboon, P. Charnkeitkong, X. Feng, Equilibrium isotherm models for adsorption of zinc (II) ion from aqueous solution on pulp waste, WSEAS Trans. Environ. Dev. 10 (2014) 35–47.
[32] E. Bazrafshan, A.A. Zarei, F. Kord Mostafapour, Biosorption of cadmium from aqueous solutions by *Trichoderma fungus*: Kinetic, thermodynamic, and equilibrium study, Desalin. Water Treat. 57 (2016) 14598–14608.
[33] R. Jiang, J. Tian, H. Zheng, J. Qi, S. Sun, X. Li, A novel magnetic adsorbent based on waste litchi peels for removing Pb(II) from aqueous solution, J. Environ. Manage. 155 (2015) 24–30.
[34] Y. Jiang, F. Li, G. Ding, Y. Chen, Y. Liu, Y. Hong, P. Liu, X. Qi, L. Ni, Synthesis of a novel ionic liquid modified copolymer hydrogel and its rapid removal of Cr(VI) from aqueous solution, J. Colloid Interface Sci. 455 (2015) 125–133.
[35] X. Sun, L. Yang, Q. Li, Z. Liu, T. Dong, H. Liu, Polyethylenimine-functionalized poly(vinyl alcohol) magnetic microspheres as a novel adsorbent for rapid removal of Cr(VI) from aqueous solution, Chem. Eng. J. 262 (2015) 101–108.
[36] I. Ghodbane, O. Hamdaoui, Removal of mercury(II) from aqueous media using eucalyptus bark: Kinetic and equilibrium studies, J. Hazard. Mater. 160 (2008) 301–309.
[37] Q. Fu, Y. Deng, H. Li, J. Liu, H. Hu, S. Chen, T. Sa, Equilibrium, kinetic and thermodynamic studies on the adsorption of the toxins of Bacillus thuringiensis subsp. Kurstaki by clay minerals, Appl. Surf. Sci. 255 (2009) 4551–4557.
[38] J. Su, H-f. Lin, Q-P. Wang, Z-M. Xie, Z-l. Chen, Adsorption of phenol from aqueous solutions by organomontmorillonite, Desalination 269 (2011) 163–169.